

A Quasi-Global Evaluation System for Satellite-Based Surface Soil Moisture Retrievals

Wade T. Crow, *Member, IEEE*, Diego G. Miralles, and Michael H. Cosh

Abstract—A recently developed data assimilation technique offers the potential to greatly expand the geographic domain over which remotely sensed surface soil moisture retrievals can be evaluated by effectively substituting (relatively plentiful) rain-gauge observations for (less commonly available) ground-based soil moisture measurements. The technique is based on calculating the Pearson correlation coefficient (R_{value}) between rainfall errors and Kalman filter analysis increments realized during the assimilation of a remotely sensed soil moisture product into the antecedent precipitation index (API). Here, the existing R_{value} approach is modified by reformulating it to run on an anomaly basis where long-term seasonal trends are explicitly removed and by calculating API analysis increments using a Rauch-Tung-Striebel smoother instead of a Kalman filter. This reformulated approach is then applied to a number of Advanced Microwave Scanning Radiometer soil moisture products acquired within three heavily instrumented watershed sites in the southern U.S. R_{value} -based evaluations of soil moisture products within these sites are verified based on comparisons with available ground-based soil moisture measurements. Results demonstrate that, without access to ground-based soil moisture measurements, the R_{value} methodology can accurately mimic anomaly correlation coefficients calculated between remotely sensed soil moisture products and soil moisture observations obtained from dense ground-based networks. Sensitivity results also indicate that the predictive skill of the R_{value} metric is enhanced by both proposed modifications to its methodology. Finally, R_{value} calculations are expanded to a quasi-global (50° S– 50° N) domain using rainfall measurements derived from the Tropical Rainfall Measurement Mission Precipitation Analysis. Spatial patterns in calculated R_{value} fields are compared to regions of strong land–atmosphere coupling and used to refine expectations concerning the global distribution of land areas in which remotely sensed surface soil moisture retrievals will contribute to atmospheric forecasting applications.

Index Terms—Data assimilation, land surface modeling and ground validation, microwave radiometer, soil moisture.

I. INTRODUCTION

A WIDE range of remote sensing retrieval strategies have been applied to routinely estimate surface soil moisture magnitudes from satellite-based instrumentation (see, e.g., [2], [23], [26], [35], and [37]). Most approaches provide soil moisture estimates at a relatively coarse spatial scale

Manuscript received April 21, 2009; revised November 12, 2009. Date of publication March 8, 2010; date of current version May 19, 2010.

W. T. Crow and M. H. Cosh are with the Hydrology and Remote Sensing Laboratory (HRSR), Agricultural Research Service, U.S. Department of Agriculture, Beltsville, MD 20705 USA (e-mail: Wade.Crow@ars.usda.gov; Michael.Cosh@ars.usda.gov).

D. G. Miralles was with the Hydrology and Remote Sensing Laboratory (HRSR), Agricultural Research Service, U.S. Department of Agriculture, Beltsville, MD 20705 USA. He is now with the Department of Hydrology, Vrije University, Amsterdam, The Netherlands (e-mail: diego.miralles@fsl.vu.nl).

Digital Object Identifier 10.1109/TGRS.2010.2040481

(> 10 – 30 km), and practical difficulties associated with the validation of such coarse-resolution products using ground-based instruments have limited the amount of performance feedback information available to soil moisture algorithm developers concerning the accuracy (and ultimate value) of their products [5], [7], [32]. Relative to ground-based soil moisture probes, ground-based rainfall gauges are inexpensive, easy to maintain, and more readily scalable and have already been widely installed over vast continental regions. For instance, within the contiguous U.S. (CONUS), the number of available rain gauges ($\sim 15\,000$) [16] is several orders of magnitude greater than the number of operational network stations currently measuring soil moisture (~ 200) [19]. Given the obvious connection between rainfall and subsequent soil moisture, it should be possible to leverage relatively abundant rain-gauge observations to indirectly evaluate the accuracy of remotely sensed surface soil moisture retrievals.

Recent work has made substantial progress in this direction. In particular, Crow *et al.* [7], [8] and Loew *et al.* [22] develop and/or apply an evaluation approach for surface soil moisture retrievals that effectively substitutes rain-gauge measurements for ground-based soil moisture observations. This approach is based on evaluating the correlation coefficient (R_{value}) between antecedent rainfall errors and analysis increments realized during the Kalman-filter-based assimilation of remotely sensed soil moisture products into a water-balance model. Because it does not require ground-based soil moisture measurements, it enables the spatial expansion of potential soil moisture validation locations from localized sites containing sufficiently dense ground-based soil moisture networks (see, e.g., [4], [19], [30], [31], and [36]) to much larger continental-scale regions containing adequate rain-gauge coverage.

Despite this progress, the baseline R_{value} approach (and previous applications of it) have been limited in several important regards. For example, R_{value} calculations have been based on a Kalman filtering methodology to assimilate raw remote sensing retrievals. The reanalysis (i.e., non-real-time) nature of the R_{value} calculation makes the use of a filtering framework potentially suboptimal. Generally, better data assimilation (DA) results can be obtained by implementing smoothing techniques in which model state predictions are updated by both past and future observations [10]. In addition, the assimilation of remotely sensed retrievals possessing a unique seasonal climatology (relative to, for example, the climatology of the assimilation model) can potentially confound the interpretation of R_{value} .

This analysis will address these shortcomings by modifying the R_{value} methodology. First, the R_{value} methodology will be altered to operate on an anomaly basis where climatological expectations in soil moisture and precipitation have been

explicitly removed. This transformation allows R_{values} to solely reflect the ability of a soil moisture product to capture actual soil moisture anomalies (relative to a given climatology) and not simply mimic seasonal soil moisture cycles. This distinction is critical for key land DA applications, like the initialization of atmospheric prediction models, where the added value of soil moisture remote sensing observations is based on their ability to capture anomalies relative to climatological expectations [9]. Second, because it is essentially a reanalysis-type exercise performed on retrospective data sets, the R_{value} methodology has been modified to be based on a Rauch–Tung–Striebel (RTS) smoother [27]. The RTS smoother provides a more appropriate estimation methodology for reanalysis-based increments than previous applications of the Kalman filter [10], [11]. These methodological changes enhance the utilization of information embedded in remotely sensed soil moisture products. Consequently, their implementation within the R_{value} methodology should provide a more robust evaluation of remotely sensed soil moisture products.

In addition to these methodological modifications, this analysis will also expand the manner in which the R_{value} metric has been applied and verified. To date, R_{value} results have not been verified through comparison with independent observations nor have they been calculated outside of relatively data-rich areas like CONUS. Crow [7] argues that R_{value} provides a robust proxy for the correlation of remotely sensed soil moisture products with true soil moisture. However, support for this assertion has been limited to results from synthetic DA experiments in which a number of potential confounding factors (e.g., seasonality, missing data, and/or autocorrelation in retrieval error) are neglected. In order to provide a more credible evaluation, R_{value} -based inferences regarding the accuracy of existing remotely sensed soil moisture products will be compared to analogous inferences obtained from dense ground-based sampling of soil moisture. Finally, using only precipitation data sets from the Tropical Rainfall Measurement Mission (TRMM) Multisatellite Precipitation Analysis (TMPA), an enhanced (and newly verified) R_{value} algorithm will be applied quasi-globally (50° S– 50° N) for the first time using remotely sensed soil moisture data sets from the Advanced Microwave Scanning Radiometer—Earth Observing System (AMSR-E) instrument.

Based on these goals, this paper is organized as follows. Section II reviews the baseline R_{value} methodology and describes the modifications introduced above. Following a description of watershed study sites in Section III and remote sensing products in Sections IV and V, Section VI presents verification results whereby inferences obtained from the application of the R_{value} approach are compared to results obtained from dense ground-based soil moisture networks. Sections VII and VIII present a quasi-global scale comparison of R_{value} results for various AMSR-E soil moisture data products—particularly within land areas identified as regions of strong land-surface/atmosphere coupling by Koster *et al.* [21].

II. R_{value} ALGORITHM

All approaches presented here are based on using daily satellite-based precipitation accumulation estimates (P^{sat}) to derive the antecedent precipitation index (API)

$$API_i = \gamma_i API_{i-1} + P_i^{\text{sat}} \quad (1)$$

where γ is the unitless API coefficient and i is a daily time index. Unless otherwise specified, γ is assumed equal to a globally constant value of 0.85. Higher quality daily rainfall accumulations derived from the retrospective correction of P^{sat} using ground-based rain gauges (P^{gauge}) must also be available but are reserved for benchmarking purposes. Values of API and P will be given in units of millimeter water depth.

A. Baseline Approach

The baseline R_{value} approach in [8] is based on the assimilation of remotely sensed soil moisture retrievals (θ_{RS} in volumetric soil moisture units of $\text{m}^3 \cdot \text{m}^{-3}$) into (1) using a Kalman filter

$$API_{\text{KF}_i}^{+} = API_{\text{KF}_i}^{-} + K_i [\theta_{\text{RS}_i} - H(API_{\text{KF}_i}^{-})] \quad (2)$$

where i is a daily time index and “ $-$ ” and “ $+$ ” denote API values before and after Kalman filter updating, respectively. The observation operator H is a simple time-constant linear function

$$H(API_{\text{KF}_i}^{-}) = a + b API_{\text{KF}_i}^{-} \quad (3)$$

whose intercept parameter a ($\text{m}^3 \cdot \text{m}^{-3}$) and slope parameter b ($\text{m}^3 \cdot \text{m}^{-3} \cdot \text{mm}^{-1}$) are obtained through a least squares regression of API, calculated via (1) using P^{gauge} and no Kalman filter updating, against θ_{RS} . Such regression implicitly assumes that the effective depth of API predictions (determined by the assumed magnitude of γ) and θ_{RS} are approximately equal. Because fitted values of a and b vary according to land cover conditions, this regression must be calculated separately for each geographic domain over which the R_{value} approach is applied (see Section V for more details).

The Kalman gain K ($\text{m}^{-3} \cdot \text{m}^3 \cdot \text{mm}$) in (2) is then given by

$$K_i = b T_{\text{KF}_i}^{-} / (b^2 T_{\text{KF}_i}^{-} + S) \quad (4)$$

where $T_{\text{KF}_i}^{-}$ (mm^2) is the background error variance in API_{KF} forecasts and S ($\text{m}^6 \cdot \text{m}^{-6}$) is the error variance in θ_{RS} retrievals. At measurement times, T_{KF}^{-} is updated following

$$T_{\text{KF}_i}^{+} = (1 - b K_i) T_{\text{KF}_i}^{-}. \quad (5)$$

Between measurements and the updating of API and T via (2) and (5), API is forecasted in time using P^{sat} and (1). The updated model forecast error T_{KF}^{+} is also forecasted as

$$T_{\text{KF}_i}^{-} = \gamma_i^2 T_{\text{KF}_{i-1}}^{+} + Q \quad (6)$$

where Q (mm^2) relates the variance added to an API forecast as it is propagated from time $i-1$ to i . Values of Q and S are calibrated through the statistical analysis of filter innovations

$$\nu_{\text{KF}_i} = [\theta_{\text{RS}_i} - H(API_{\text{KF}_i}^{-})] / (b^2 T_{\text{KF}_i}^{-} + S)^{0.5}. \quad (7)$$

A properly constructed linear filter should yield a ν_{KF} time series that is serially uncorrelated [14]. Here, a simple tangent-linear optimization algorithm is used to iteratively vary the Q/S ratio until this constraint is satisfied.

Updates to API given by (2) in the course of assimilating a particular remotely sensed soil moisture product are referred to as “analysis increments”

$$\begin{aligned}\delta_{KF_i} &= API_{KF_i}^+ - API_{KF_i}^- \\ &= K_i [\theta_{RS_i} - H(API_{KF_i}^-)].\end{aligned}\quad (8)$$

If θ_{RS} has appreciable skill in detecting soil moisture temporal variations, values of δ_{KF} will correlate with near-past errors in precipitation anomalies ($P^{sat} - P^{gauge}$). Following [7], both δ_{KF} and $P^{sat} - P^{gauge}$ are summed within a series of nonoverlapping windows of length N day(s), and a correlation coefficient is calculated between the N -day sums of δ_{KF} and $P^{sat} - P^{gauge}$. The negative of this correlation coefficient is referred to as the R_{value} metric for a particular θ_{RS} product. Higher R_{value} indicates increased efficiency in the filtering of error in API predictions arising from random noise in P^{sat} estimates. In this way, the R_{value} metric measures the degree to which the assimilation of θ_{RS} adds value to model-based estimates of surface soil moisture—above and beyond the baseline case of simply driving (1) with P^{sat} . One consequence of this interpretation is that R_{value} should have a direct one-to-one relationship with the correlation coefficient between θ_{RS} and true soil moisture [7]. Using the simple modeling approach in (1), we will attempt to verify this relationship and clarify accuracy requirements for P^{gauge} measurements forming the basis of the R_{value} evaluation approach.

B. Anomaly Modification

Crow *et al.* [7], [8] use the baseline approach described earlier to generate 1° latitude/longitude R_{value} maps, and they argue that these maps constitute a robust proxy for Pearson’s correlation coefficient between θ_{RS} and true soil moisture (as acquired, e.g., from a dense ground-based soil moisture network). Such correlations are sensitive to both the skill of retrievals with regard to short-term soil moisture anomalies and their ability to capture typical soil moisture seasonal cycling. One consequence of this dual sensitivity is that a given soil moisture product can exhibit a relatively high correlation coefficient (and, thus, high R_{value}) based solely on accurately mimicking climatological seasonal variations in soil moisture while possessing little or no skill in capturing shorter-term anomalies. Most soil moisture DA systems are based on scaling the observed soil moisture into a model’s unique soil moisture climatology—ideally on a seasonal or monthly basis (see, e.g., [12])—prior to its assimilation. As a result, accurately capturing soil moisture seasonal cycles in a remotely sensed product is of relatively little value. For many DA applications, a more important reflection of product value is skill with regard to detecting soil moisture anomalies relative to an expected annual cycle [9].

To this end, we propose decomposing raw precipitation and soil moisture time series into their climatology and anomaly components

$$\hat{\theta}_{RS_i} = \theta_{RS_i} - \bar{\theta}_{RS_{DOY}} \quad (9)$$

$$\hat{P}_i^{sat} = P_i^{sat} - \bar{P}_{DOY}^{sat} \quad (10)$$

$$\hat{P}_i^{gauge} = P_i^{gauge} - \bar{P}_{DOY}^{gauge} \quad (11)$$

where $\bar{\theta}_{RS_{DOY}}$, \bar{P}_{DOY}^{sat} , and \bar{P}_{DOY}^{gauge} are climatological expectations for a given day of the year (DOY) and $\hat{\theta}_{RS_i}$, \hat{P}_i^{sat} , and \hat{P}_i^{gauge} are anomalies relative to these expectations experienced on a particular day i . Expectations are calculated by simple linear averaging within a 31-day moving window centered on the particular DOY corresponding to i and the entire (multiyear) historical data set for each variable.

Because the baseline R_{value} analysis in Section II-A is fully linear, raw values of θ_{RS} and P^{sat} appearing in (1)–(8) can be substituted with their anomaly equivalents without any loss of validity. In particular, (1) can be modified to produce anomaly API forecasts

$$\widehat{API}_i = \gamma_i \widehat{API}_{i-1} + \hat{P}_i^{sat} \quad (12)$$

which are then updated using $\hat{\theta}_{RS}$ to produce anomaly analysis increments

$$\widehat{\delta}_{KF_i} = \hat{K}_i [\hat{\theta}_{RS_i} - H(\widehat{API}_{KF_i}^-)] \quad (13)$$

where \hat{K} is based on substituting anomaly-based values of T and S (\hat{T} and \hat{S}) into (4). Analysis increments obtained from (13) and the rainfall anomaly difference $\hat{P}^{sat} - \hat{P}^{gauge}$ are both summed within nonoverlapping N -day windows, and R_{value} is estimated from the negative of their Pearson’s correlation coefficient. The process mimics the baseline version perfectly, except that R_{value} results now reflect skill in θ_{RS} with respect to only soil moisture anomaly detection.

C. RTS Smoother Modification

The RTS smoother is based on adding a second backward-propagating update to the Kalman filter analysis that incorporates information contained in observations made after the time of update. Because a filter-based update is limited to consider only prior observations, this backward propagation allows for the more efficient use of information embedded in soil moisture retrievals. Furthermore, because our R_{value} methodology is essentially a reanalysis-type analysis, there are no practical barriers (e.g., the need for real-time results) to the implementation of a smoothing approach.

After the complete calculation and calibration of Kalman-filter-based increments (now based on climatological anomalies following Section II-B), the RTS smoother propagates information backward in time starting with the final conditions of

$$\widehat{API}_{RTS} = \widehat{API}_{KF}^+ \quad (14)$$

$$\hat{T}_{RTS} = \hat{T}_{KF}^+. \quad (15)$$

The time-backward propagation of these variables is given by

$$\widehat{API}_{RTS_i} = \widehat{API}_{KF_i}^+ + A_i (\widehat{API}_{RTS_{i+1}} - \widehat{API}_{KF_{i+1}}^-) \quad (16)$$

$$\hat{T}_{RTS_i} = \hat{T}_{KF_i}^+ + A_i^2 (T_{RTS_{i+1}} - \hat{T}_{KF_{i+1}}^-) \quad (17)$$

where

$$A_i = \gamma \hat{T}_{KF_i}^+ / \hat{T}_{KF_{i+1}}^-. \quad (18)$$

Upon propagation of this second smoothing step, the total analysis increment becomes

$$\widehat{\delta}_{\text{RTS}_i} = \widehat{\delta}_{\text{KF}_i} + A_i \left(\widehat{\text{API}}_{\text{RTS}_{i+1}} - \widehat{\text{API}}_{\text{KF}_{i+1}}^- \right) \quad (19)$$

where $\widehat{\delta}_{\text{KF}}$ is given by (13). R_{value} is then the negative of Pearson's correlation coefficient between N -day sums of $\widehat{\delta}_{\text{RTS}}$ and $\widehat{P}^{\text{sat}} - \widehat{P}^{\text{gauge}}$.

III. WATERSHED SITES

The R_{value} approach described in Section II will be evaluated based on soil moisture and rainfall observations available within three separate U.S. Department of Agriculture (USDA) Agricultural Research Service (ARS) experimental watersheds. Each watershed contains a dense ground-based soil moisture network constructed to facilitate its participation in AMSR-E soil moisture validation activities [19]. As a result, these three watersheds provide an opportunity to assess the performance of the R_{value} metric over a range of land surface and climate conditions.

A. LR, GA

The 334-km² Little River (LR) Experimental Watershed is located in southern Georgia. The USDA-ARS Southeast Watershed Research Laboratory at Tifton, GA, has been collecting hydrologic and climatic data in the watershed since 1968. Land use is a mixture of pasture and forage production, row-crop agriculture (primarily summertime cotton and peanuts), and upland and riparian forests. The watershed topography is characterized by rolling hills and gentle slopes. Climate is humid, with a mean annual precipitation of around 1200 mm—the majority of which occurs during short-duration but high-intensity convective thunderstorms. Rainfall and soil moisture ground data sets are based on measurements made at 29 separate stations within the watershed. For more details on the watershed and its observational networks, see [3], [4], and [19].

B. LW, OK

The 611-km² Little Washita (LW) Watershed is located in southwestern Oklahoma. The watershed has served as the site for a large number of soil erosion studies since 1936 and hydrological experiments since 1961. Land use is dominated by rangeland and pastures, with significant areas of winter wheat cultivation within the western half of the watershed. The topography is generally flat, with a maximum relief of less than 200 m. Climate is subhumid, with a mean annual precipitation of 760 mm and a mean annual temperature of 16 °C. The watershed experiences strong seasonal variations, with hot and dry summers separated from cold and dry winters by relatively wet periods in the spring and fall. The ground data used here were acquired at 42 rain gauges and 20 soil moisture stations within the study area. Measurements are made as part of the ARS Micronet operated and maintained by the USDA-ARS Grazinglands Research Laboratory in cooperation with Oklahoma State University and the Oklahoma Climatological

Survey. For more details on the LW Watershed and these observations, see [1], [5], [19], and <http://ars.mesonet.org>.

C. WG, AZ

The 150-km² Walnut Gulch (WG) Experimental Watershed is located in southeastern Arizona. The USDA-ARS Southwest Watershed Research Center in Tucson, AZ, has been collecting rainfall data at the site since 1956 and soil moisture since 1996. Land cover is generally brush and short-grass rangeland. Elevation within the watershed ranges from 1250 to 1585 m above sea level. Located in a semiarid climate zone, the precipitation regime is dominated by the North American monsoon system, with about 60% of the annual rainfall associated with summer convective storms. The mean annual rainfall is 350 mm, and the mean annual temperature is 18 °C. Precipitation data are collected at 82 stations, while the soil moisture is recorded at 19 separate locations. For more details on the WG Experimental Watershed and these observations, see [6], [15], [19], and [29].

IV. REMOTE SENSING DATA

Remotely sensed soil moisture retrievals are based on five separate products derived from a range of passive microwave brightness temperature (T_B) observations made by the AMSR-E sensor aboard the National Aeronautics and Space Administration (NASA) Aqua satellite. The AMSRE_{NASA} product is the official NASA AMSR-E Level 3 soil moisture product [25] derived from application of the dual polarization algorithm described in [23] to H- and V-polarized AMSR-E X-band (10.6-GHz) T_B observations. The AMSRE_{USDA} product (developed at the USDA Hydrology and Remote Sensing Laboratory by T. J. Jackson and R. Bindlish) is based on X-band T_B observations as well but uses the single-channel (H-polarization only) algorithm of Jackson [18]. The AMSRE_{VU} product (developed at the Vrije University of Amsterdam (VU) by R.A.M. de Jeu and T. Holmes in collaboration with M. Owe at the NASA Goddard Space Flight Center) applies the algorithm of Owe *et al.* [26] to dual-polarized C-band (6.9-GHz) T_B and falls back to X-band T_B in areas of significant C-band radio-frequency interference (RFI) over the U.S. and Japan [24]. A fourth product (AMSRE_{SWI}) is based on the application of the soil wetness index (SWI) approach [33] to the AMSR-E T_B measurements. Here, SWI is simply the difference of AMSR-E H-polarized T_B observations at 89 and 18.7 GHz. A final soil moisture product (AMSRE_{COMB}) is obtained from arithmetic averaging of the AMSRE_{USDA}, AMSRE_{VU}, and AMSRE_{NASA} products. To ensure equal weighting, the AMSRE_{USDA}, AMSRE_{VU}, and AMSRE_{NASA} soil moisture products are linearly normalized to the same mean and standard deviation prior to this averaging. For all five products (AMSRE_{SWI}, AMSRE_{NASA}, AMSRE_{USDA}, AMSRE_{VU}, and AMSRE_{COMB}), soil moisture retrievals obtained from ascending (1:30 P.M.) and descending (1:30 A.M.) AMSR-E overpasses are analyzed separately.

Two separate satellite-based rainfall data sets produced by TMPA [17] are also utilized. Unless otherwise stated, P^{sat} is based on the real-time TRMM 3B40RT product calculated

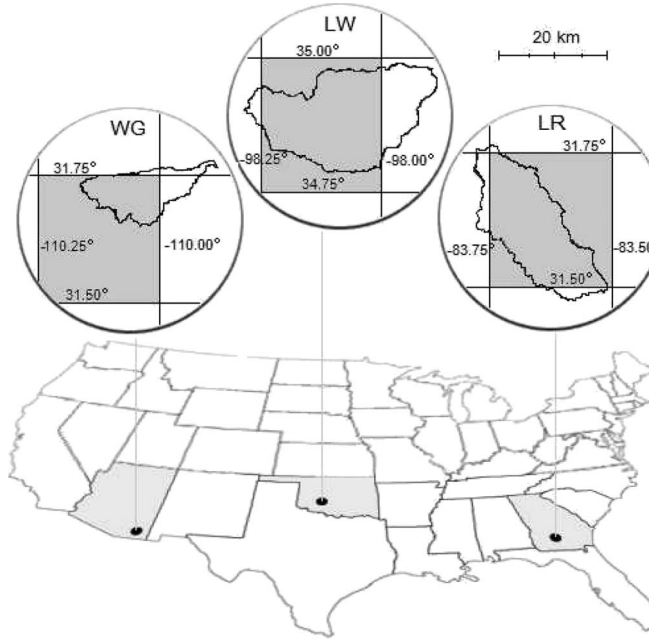


Fig. 1. Location and boundaries for the WG (AZ), LW (OK), and LR (GA) USDA-ARS experimental watersheds. The shaded square is the quarter-degree grid cell used to approximate each watershed.

using a combination of microwave-only satellite data derived from a number of sensors [17]. In contrast, the TRMM 3B42 product is computed by combining these passive microwave estimates with microwave-calibrated infrared (IR) estimates and a retrospective correction based on monthly rain-gauge data [17]. Our use of the TRMM 3B42 product will vary with context. For the watershed verification analysis in Section VI, it, along with TRMM 3B40RT, will be used for P^{sat} . For the quasi-global analysis in Sections VII and VIII, it will be used exclusively for the benchmark P^{gauge} rainfall product.

V. APPROACH

The study period for the entire analysis is from February 2, 2002, to December 31, 2007. However, because AMSR-E observations did not become available until June 2002, the first four months of this period are reserved for spinning up the API model. All API modeling is based on a daily time step. Unless otherwise noted, a window length of $N = 5$ days is used, and a minimum threshold of two observations per window is enforced. Time windows failing this threshold are removed from the analysis and not used to calculate R_{value} . Daily TRMM 3B40RT and 3B42 rainfall accumulation estimates are extracted from the quarter-degree latitude/longitude grid box that most closely approximates the spatial extent of each watershed (see Fig. 1). Likewise, retrievals for the five remotely sensed soil moisture products ($\text{AMSRE}_{\text{NASA}}$, $\text{AMSRE}_{\text{USDA}}$, AMSRE_{VU} , $\text{AMSRE}_{\text{SWI}}$, and $\text{AMSRE}_{\text{COMB}}$) are extracted from gridded quarter-degree data products for each of the soil moisture data sets. Relative to the LR and LW watersheds, the best quarter-degree grid fit for the WG watershed is still a poor spatial approximation of the actual watershed (Fig. 1). Therefore, for the WG site, a sensitivity analysis was performed to determine

the impact of extracting WG $\text{AMSRE}_{\text{USDA}}$ and $\text{AMSRE}_{\text{NASA}}$ retrievals from individual swath-based footprints instead of a pregridded quarter-degree analysis. Because results from this test indicate little or no impact on subsequent R_{value} results and some AMSR-E soil moisture products are not readily available in swath format, extraction from quarter-degree gridded data products is retained for our multi-product analysis at the WG site. In addition, to allow for direct comparisons between different soil moisture products, a particular quarter-degree grid (for a given overpass) is included in the analysis only if it contains a viable soil moisture retrieval for all five soil moisture products. As noted previously, retrievals from ascending and descending AMSR-E overpasses are considered separately.

For watershed verification results (Section VI), the API modeling day is defined as the 24-h period starting at midnight Central Standard Time (CST). As noted in Section III, each watershed contains its own dense rain-gauge network. Simple arithmetic averaging is applied to spatially aggregate daily rainfall accumulation values from individual rain gauges within each watershed into a mean daily accumulation for the watershed. These spatially averaged values are then used for P^{gauge} . Based on [19], weighted averages developed through Thiessen polygons are employed to upscale ground-based soil moisture measurements from individual stations to the entire watershed. In order to match AMSR-E overpass times, only ground-based soil moisture observations taken at 1:30 P.M. or 1:30 A.M. local solar time are considered. Due to a disruption in the availability of ground-based soil moisture during late 2007, the watershed analysis in Section VI ended on July 25, August 26, and September 23, 2007, for the WG, LW, and LR watersheds, respectively. Values of a and b in (3) are equal to slope and intercept parameters derived from least squares linear regression of an API time series, derived using P^{gauge} in (1) and no Kalman filtering updating, to AMSR-E surface soil moisture products. This fitting is based on data from the entire analysis period (2002 and 2007), and separate parameters are obtained for each AMSR-E soil moisture product at every watershed site.

The quasi-global (50° S– 50° N) results in Section VII are based on a different temporal and spatial gridding. Prior to any subsequent processing, precipitation and soil moisture remote sensing products are aggregated onto a 1° latitude/longitude spatial grid. Daily precipitation depths P^{sat} and P^{gauge} are based on the total rainfall accumulation observed between 12 and 12 UTC, and the soil moisture values for the same day are taken from any ascending or descending AMSR-E retrieval acquired during a period shifted 12 hours into the future (0–24 UTC). This shift is done to maximize the probability that the soil moisture retrieval will occur after a particular rainfall event—as is implicitly assumed in the R_{value} approach (see Section II). At the global scale, P^{sat} and P^{gauge} are always derived from TRMM 3B40RT and TRMM 3B42 results, respectively. Note this difference relative to the watershed approach described before, where both TRMM 3B42 and 3B40RT are used for P^{sat} , and P^{gauge} is derived from local rain-gauge networks. For the global-scale analysis, parameters a and b in (3) are derived as in the watershed case described earlier except based on linear least squares fitting applied separately to each 1° grid box.

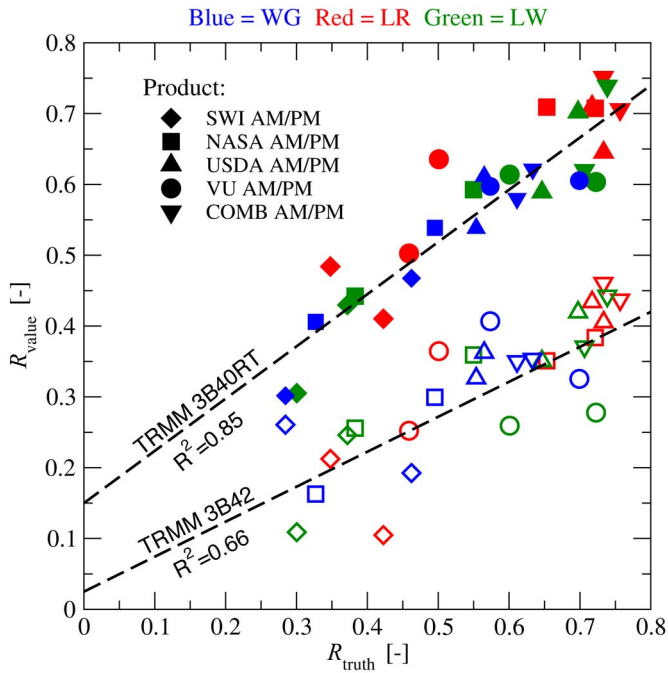


Fig. 2. Based on the anomaly and RTS smoother modifications described in Section II, the relationship between R_{truth} and R_{value} for all AMSR-E soil moisture products (see Section IV) within the three watershed sites (WG is blue, LR is red, and LW is green). Results illustrate the use of both (open symbols) TRMM 3B42 and (filled symbols) 3B40RT precipitation products as P^{sat} .

VI. WATERSHED VERIFICATION RESULTS

For the three watersheds described in Section III, Fig. 2 shows R_{value} watershed results with Pearson's correlation coefficients between daily AMSR-E soil moisture products and daily watershed-scale soil moisture estimates obtained from the spatial averaging of high-density soil moisture ground networks. These ground-based correlations, referred to as R_{truth} , reflect the type of high-quality evaluation that is currently available within only a small number of heavily instrumented watershed sites. The point cloud in Fig. 2 is created by lumping results from all three USDA-ARS watersheds (WG, LW, and LR) and all five AMSR-E soil moisture products (AMSRE_{SWI}, AMSRE_{NASA}, AMSRE_{USDA}, AMSRE_{VU}, and AMSRE_{COMB}). In addition, results are shown for the use of both TRMM 3B42 (open symbols) and TRMM 3B40RT (filled symbols) precipitation products as P^{sat} . Unless otherwise noted, results are based on implementation of both the anomaly and RTS smoother modifications described in Section II. For consistency with the anomaly-based R_{value} calculations, the R_{truth} correlation coefficient is also sampled after seasonal cycles have been removed from both the remotely sensed and ground-based soil moisture observations.

The use of TRMM 3B40RT data as P^{sat} leads to a high correlation between R_{truth} and R_{value} ($R^2 = 0.85$), suggesting that R_{value} can accurately mimic the correlation-based evaluation of soil moisture products without any reliance on ground-based soil moisture observations (see the filled symbols in Fig. 2). This result verifies the underlying R_{value} approach by demonstrating its ability to accurately reproduce validation results obtained from very dense ground-based soil moisture networks. As discussed in Section II, the R_{value} results in Fig. 2 are based on a—temporally and spatially constant—choice of

$\gamma = 0.85$ for API modeling in (1). However, varying γ between 0.80 and 0.90 led to only very minor changes in the observed correlation between R_{truth} and R_{value} .

Despite the obvious simplicity of the API-based modeling approach in (1), the majority of the observed scatter in Fig. 2 appears to be an attributable simple random sampling error and not any underlying incompatibility between R_{truth} and R_{value} . For example, 1σ sampling uncertainty in the estimated correlation coefficient used for R_{value} is responsible for about 75% of the observed root-mean-square (rms) scatter around the TRMM 3B40RT least squares regression line in Fig. 2 [34]. Consequently, it appears unlikely that the observed fit in Fig. 2 can be substantially improved via the application of more complex soil water-balance models. The observed correlations in Fig. 2 are also degraded by the presence of sampling error in the daily watershed-scale soil moisture estimates derived by Jackson *et al.* [19] from ground-based observations and used here to calculate R_{truth} . However, structural and sampling uncertainties are likely much larger for R_{value} estimates relative to comparably direct R_{truth} calculations. Therefore, the presence of significant correlation between independently acquired R_{value} and R_{truth} in Fig. 2 strongly implies that the ground-based observations of Jackson *et al.* [19] are accurately representing watershed-scale soil moisture dynamics.

The use of the higher accuracy TRMM 3B42 rainfall product, instead of TRMM 3B40RT, as P^{sat} leads to a reduction in calculated R_{value} (compare the filled and open symbols in Fig. 2). This reduction reflects the relationship noted by Crow [7], where by higher (lower) accuracy P_{sat} rainfall products lead to lower (higher) R_{value} magnitudes. Note that R_{value} is a metric of added value and can therefore be increased through either of the following ways: 1) the improvement of soil moisture retrievals or 2) the degradation of competing soil moisture estimates obtained from water-balance modeling and remotely sensed rainfall [7]. In Fig. 2, the lower R_{value} associated with TRMM 3B42 reflects the fact that a better rainfall product makes it incrementally more difficult for a soil moisture product to provide added skill. In addition, the transition to the TRMM 3B42 product reduces the observed R^2 correlation between R_{truth} and R_{value} from 0.85 to 0.66.

As noted previously, the results in Fig. 2 and Table I are based on adopting both the anomaly and RTS smoother modifications discussed in Section II-B and C, respectively. In order to motivate these modifications, Table I presents summary statistics (i.e., the R^2 between R_{truth} and R_{value} and the average R_{value} calculated across all sites) for analogous results calculated with and without these modifications. For consistency, R_{truth} benchmark results are obtained for either raw or anomaly soil moisture times series, depending on whether they are being compared to raw or anomaly-based R_{value} results. The raw/KF results in Table I reflect the baseline R_{value} approach applied in [7] and [8]. Regardless of whether TRMM 3B40RT or 3B42 rainfall is used as P^{sat} , the implementation of each modification (alone or in combination) improves the performance of the R_{value} metric. Note the clear increase in the R^2 correlation between R_{truth} and R_{value} for the fully modified (anomaly/RTS) case relative to the original (Raw/KF) approach used in [7] and [8]. Consequently, modifications to the R_{value} methodology described in Section II appear to produce a more reliable evaluation metric.

TABLE I
OBSERVED CORRELATION BETWEEN R_{value} AND GROUND-BASED R_{truth} (R^2) AND AVERAGE R_{value} (\bar{R}_{value}) IN FIG. 2 BASED ON THE FOLLOWING: THE RAINFALL PRODUCT USED FOR P^{sat} (TRMM 3B42 OR 3B40RT), THE CHOICE OF DA METHOD (KF OR RTS SMOOTHER), AND THE TYPE OF TIME-SERIES VARIABLE EXAMINED (RAW VALUES OR ANOMALIES OBTAINED BY REMOVING A CLIMATOLOGICAL SEASONAL CYCLE)

P^{sat}	DA Method	Raw/Anomaly	R^2	\bar{R}_{value}
3B42	KF	Raw	0.46	0.25
		Anomaly	0.54	0.29
	RTS	Raw	0.45	0.26
		Anomaly	0.66	0.32
3B40RT	KF	Raw	0.65	0.48
		Anomaly	0.68	0.51
	RTS	Raw	0.68	0.53
		Anomaly	0.85	0.57

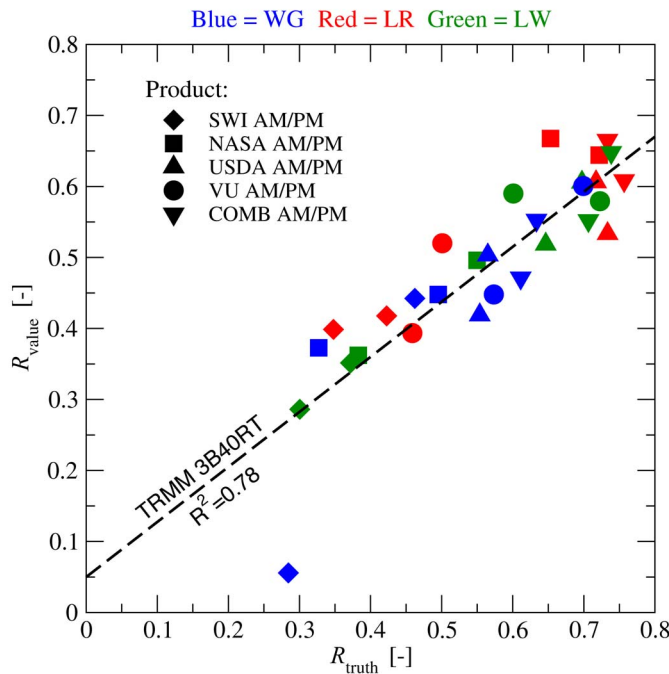


Fig. 3. Based on the anomaly and RTS smoother modifications described in Section II, the relationship between R_{truth} and R_{value} for all AMSR-E soil moisture products (see Section IV) within the three watershed sites (WG is blue, LR is red, and LW is green). Results illustrate the single case of using TRMM 3B40RT rainfall for P^{sat} and TRMM 3B42 for P^{gauge} .

VII. GLOBAL RESULTS

All R_{value} watershed verification results in Fig. 2 are based on using daily rainfall observations obtained from dense rain-gauge networks to estimate P^{gauge} . Consequently, P^{gauge} accuracies obtainable at these sites are likely unrepresentative of ground-based rainfall products available at less heavily instrumented locations. In order to estimate the impact of a reduction in P^{gauge} accuracy on Fig. 2, Fig. 3 shows the relationship between R_{value} and R_{truth} for the case of P^{gauge} acquired from the TRMM 3B42 product. Because it is gauge-corrected only at a monthly time scale using relative sparse measurements [17], the TRMM 3B42 product represents a substantial reduction in

the accuracy of P^{gauge} rainfall pentads relative to the daily rain-gauge-based pentads used for P^{gauge} in Fig. 2.

Reducing the accuracy of P^{gauge} leads to a slightly lower correlation between the calculated R_{value} and observed R_{truth} (compare the closed symbols in Figs. 2 and 3). Nevertheless, a significant level of correlation is retained ($R^2 = 0.78$). This suggests that the R_{value} approach is reliable even when global rainfall products (and not local rain-gauge observations) are used for P^{gauge} . The key to a robust R_{value} response is not precisely the absolute accuracy of the P^{gauge} product but rather the relative accuracy of the P^{gauge} versus the P^{sat} product. In areas of the world in which monthly rain-gauge observations are available for a retrospective correction of satellite-based retrievals, there appears to be a large-enough difference between the accuracy of the TRMM 3B40RT and 3B42 products to calculate a reliable R_{truth} . Unfortunately, the results in Fig. 3 provide a lesser guarantee for extremely data-poor areas in which even monthly retrospective rain-gauge correction is difficult and/or impossible to perform. One potential solution in such areas is to use an expanded 30-day window size (N) to maximize the filtering of short-term errors in P^{gauge} . However, in the case of Fig. 3, converting from a 5-day to 30-day window size actually reduces the observed correlation between R_{value} and R_{truth} from $R^2 = 0.78$ to 0.61 (not shown). This reduction appears to be in response to the reduced consistency between the (now monthly) temporal support of R_{value} estimates and remaining daily basis of R_{truth} . As a result, the use of a five-day aggregation window is retained for all future R_{value} calculations.

Using TRMM 3B42 for P^{gauge} and TRMM 3B40RT as P^{sat} , quasi-global (land areas between 50° S and 50° N) R_{value} results are calculated for each of the remotely sensed soil moisture data sets introduced in Section IV. As discussed earlier, high- R_{value} results indicate that a given soil moisture product is contributing to an improved representation of soil moisture anomalies (above and beyond the baseline obtainable using API modeling forced by TRMM 3B40RT rainfall). Fig. 4 shows variations in the average R_{value} performance of various products—grouped according to the lowest frequency AMSR-E T_B observation used to create them. Within both CONUS [Fig. 4(a)] and quasi-global [Fig. 4(b)] domains, implementation of the new RTS and anomaly-based approach leads to spatially averaged R_{value} results (indicated by open circles) that gradually rise as T_B frequency falls [Fig. 4(b)]. The slight suppression of AMSRE_{VU} R_{value} results over CONUS (relative to extrapolated expectations for a C-band product) is almost certainly due to C-band (6.9-GHz) RFI considerations that forced Owe *et al.* [26] to fall back on X-band (10.6-GHz) T_B observations over many parts of the U.S. The relative performance of A.M.- versus P.M.-based retrievals also varies from product to product. Over the quasi-global domains [Fig. 4(a)], daytime P.M. overpasses yield slightly better retrievals for the AMSRE_{NASA}, AMSRE_{USDA}, and AMSRE_{SWI} products, while nighttime A.M. overpasses are preferable for the AMSRE_{VU} product.

Fig. 4 also shows relative variations in temporally averaged R_{value} associated with different R_{value} methodologies. Over the CONUS domain [Fig. 4(a)], the transition between raw and anomaly-based R_{value} calculations (see Section II-B)

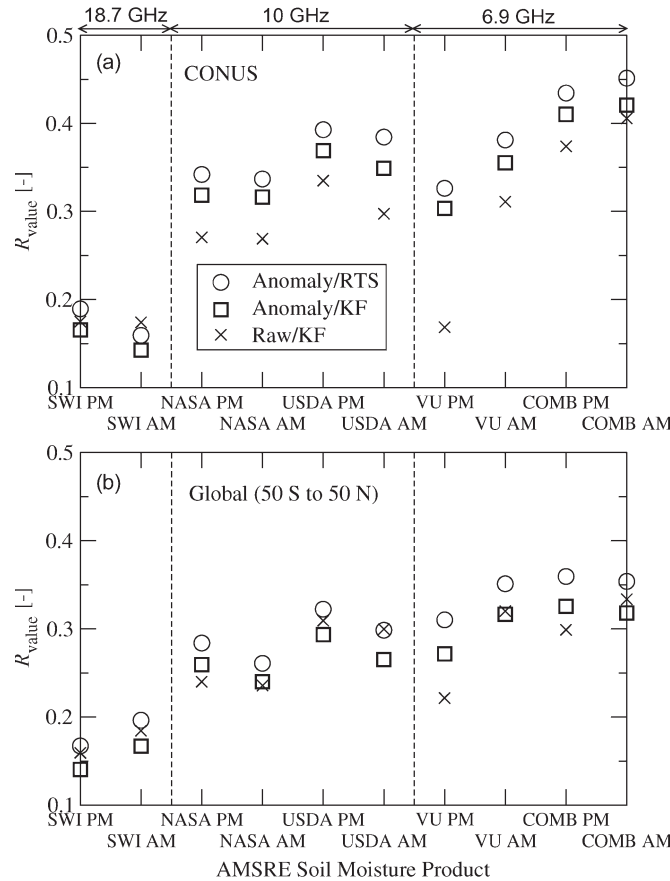


Fig. 4. Over the (a) CONUS domain and (b) all global land areas between 50° S and 50° N, the spatial average of R_{value} for the $\text{AMSRE}_{\text{SWI}}$, $\text{AMSRE}_{\text{NASA}}$, $\text{AMSRE}_{\text{USDA}}$, AMSRE_{VU} , and $\text{AMSRE}_{\text{COMB}}$ products described in Section IV. Results are horizontally organized according to the lowest frequency T_B observations utilized for each product and given for cases of implementing (“raw/KF”) neither of the modifications in Section II, (“anomaly/KF”) only the anomaly modification, and (“anomaly/RTS”) both the anomaly and RTS smoother modifications.

and the subsequent transition from a Kalman filter to an RTS smoother implementation (see Section II-C) consistently increases R_{value} for all products except $\text{AMSRE}_{\text{SWI}}$. At the quasi-global scale [Fig. 4(b)], a consistently positive impact is associated with switching to an RTS smoother; however, the impact of preprocessing data into anomalies is more erratic, with large improvements being noted for some products (e.g., the AMSRE_{VU} P.M. product) and small decreases for others (e.g., the $\text{AMSRE}_{\text{USDA}}$ A.M. and P.M. products). This variable response is tied to the accuracy of each product with regard to representing seasonal soil moisture dynamics. For example, the AMSRE_{VU} P.M. product has a known problem capturing wet/dry seasonal trends over areas of Africa (T. Holmes, personal communication). Difficulties associated with seasonal cycles can impair the ability of a given product to represent fine-scale temporal soil moisture anomalies. Consequently, implementing the anomaly-based calculation of R_{value} , in which (potentially artificial) seasonal trends are explicitly removed, leads to a large increase in calculated R_{value} . Conversely, because seasonal trends in $\text{AMSRE}_{\text{USDA}}$ predictions are relatively more accurate, their removal actually leads to a small decrease in R_{value} . In addition to these

differences in performance, the appropriateness of raw versus anomaly-based R_{value} metrics is dependent on the degree to which capturing seasonal predictions represents an important source of retrieval skill for specific applications. For many DA applications, all soil moisture products (regardless of their accuracy) are preprocessed to explicitly match a land surface model’s individual soil moisture climatology prior to being ingested. Consequently, added value in the assimilation product is derived solely from an improved representation of anomalies relative to this climatology [9]. In these cases, anomaly-based R_{value} calculations (open circles in Fig. 4) provide a more robust representation of the overall retrieval value by de-emphasizing the accurate representation of a seasonal cycle.

Complete quasi-global 1° imagery is shown in Fig. 5 for A.M. and P.M. retrievals from all AMSR-E-based soil moisture products except $\text{AMSRE}_{\text{COMB}}$. The first-order patterns seen in Fig. 5 reflect the global distribution of vegetation biome types that are amenable to microwave-based soil moisture remote sensing. High skill with regard to anomaly detection (red shading) is clearly evident in lightly-vegetated areas of the western U.S., the Iberian peninsula, the Sahel region of Africa, central Asia, southern Africa, Australia, and the Pampas region of South America. Low skill (blue shading) is identified in the rainforest regions of South America, Africa, and Indonesia, as well as densely vegetated areas in eastern North America.

In addition to these broad geographic patterns, a number of product-to-product differences can be detected. Based only on high-frequency > 10 -GHz T_B measurements, the $\text{AMSRE}_{\text{SWI}}$ algorithm demonstrates little added skill outside of sparsely vegetated areas. Much better results are obtained for all other products obtained from lower frequency T_B observations. In particular, the $\text{AMSRE}_{\text{USDA}}$ and $\text{AMSRE}_{\text{NASA}}$ products use the same AMSRE T_B band (10.6 GHz) but differ in their basis for estimating vegetation canopy opacity. While the single-polarization $\text{AMSRE}_{\text{USDA}}$ product requires ancillary vegetation information, typically derived from historical visible and near-IR remote sensing data, to estimate canopy opacity, the $\text{AMSRE}_{\text{NASA}}$ products estimate opacity directly from dual-polarization microwave T_B observations. Fig. 5 suggests that, at least for X-band products, the added ancillary data requirements of the $\text{AMSRE}_{\text{USDA}}$ product enhance the large-scale accuracy of its A.M. retrievals over Australia and western North America. Likewise, the use of dual-polarized C-band AMSRE T_B appears to provide additional skill to the AMSRE_{VU} A.M. product (relative to both the X-band $\text{AMSRE}_{\text{USDA}}$ and $\text{AMSRE}_{\text{NASA}}$ products) in areas of eastern Africa and along a broad swath of Central Asia. Note that the lack of a C-band single-polarization product in the analysis prevents a full examination of dual- versus single-polarization effects on C-band retrievals. In contrast to the product-to-product variations seen in the A.M. products, relatively little difference is observed between the $\text{AMSRE}_{\text{USDA}}$, $\text{AMSRE}_{\text{NASA}}$, and AMSRE_{VU} P.M. products—seemingly suggesting that intra-algorithm differences are more pronounced for daytime P.M. retrievals.

Fig. 5 can also be used to examine 1:30 P.M. versus 1:30 A.M. overpass differences for various products. For instance, the

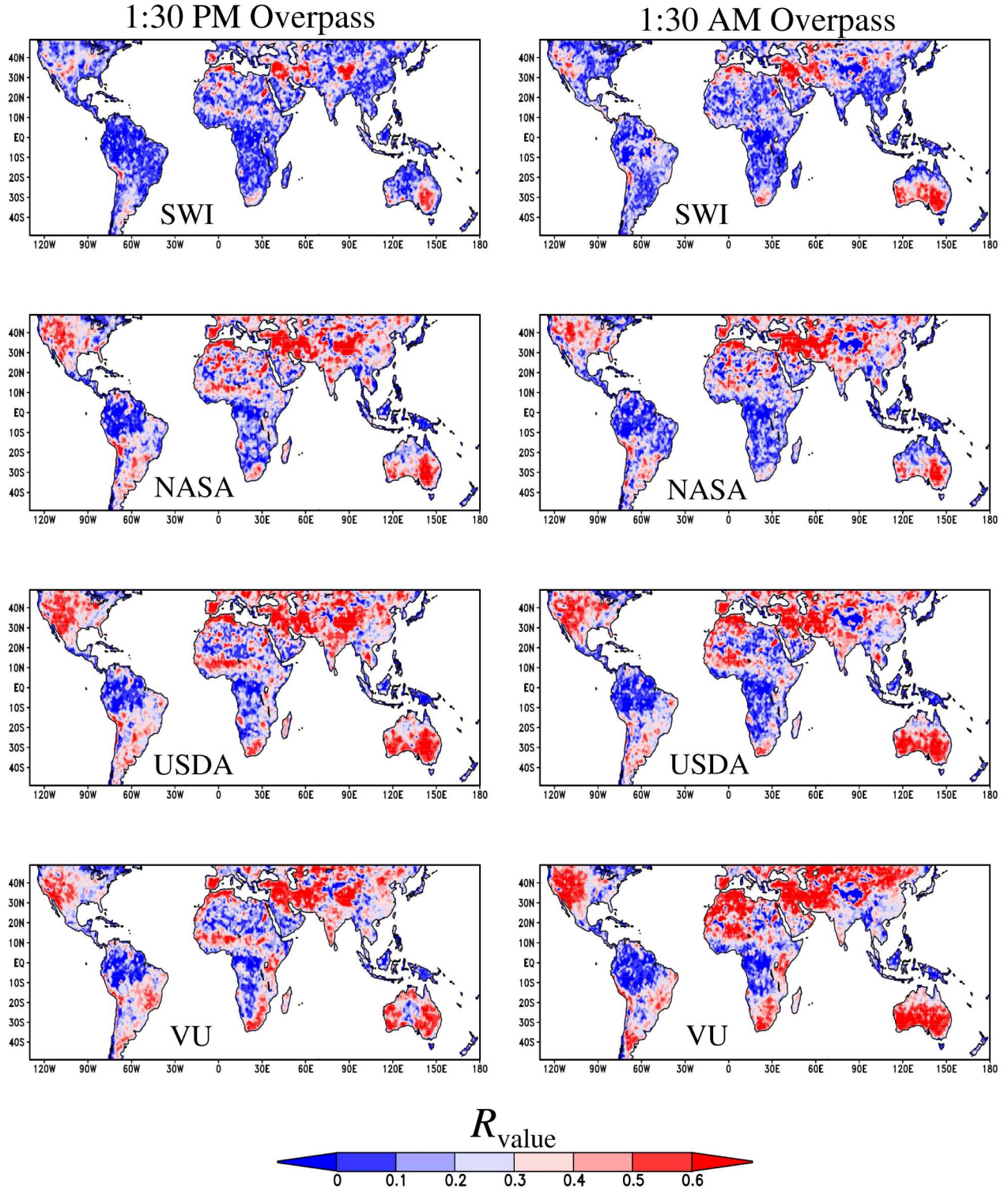


Fig. 5. Quasi-global R_{value} results for the AMSRE_{SWI}, AMSRE_{NASA}, AMSRE_{USDA}, and AMSRE_{VU} soil moisture products described in Section IV. Columns separate retrievals based on 1:30 A.M. and 1:30 P.M. local solar time AMSR-E overpasses.

AMSRE_{VU} A.M. product is superior to its P.M. counterpart over arid areas of western North America, north Africa, northeast Asia, and central Australia. Both AMSRE_{VU} and AMSRE_{USDA} products retrieve soil moisture based on surface temperature estimates obtained from 37-GHz AMSR-E T_B observations [19], [26]. These surface temperature estimates

are prone to error for daytime conditions in arid climates and are likely a significant source of uncertainty in retrievals based on 1:30 P.M. overpasses. Somewhat surprisingly given their similar approach to surface temperature estimation, an analogous A.M./P.M. contrast is not seen for the AMSRE_{USDA} results in Fig. 5. Some care should be taken in interpreting A.M.

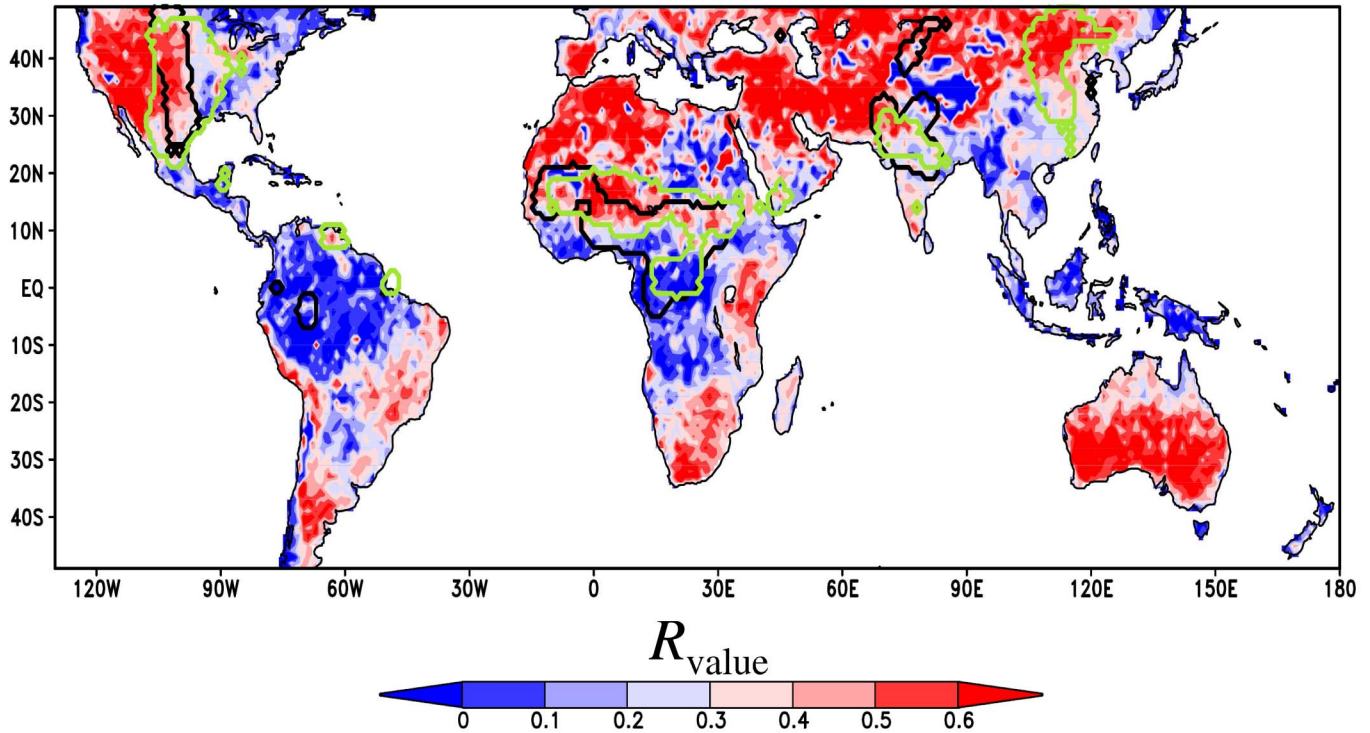


Fig. 6. Outline of GLACE [21] hot spots for (black) precipitation and (green) temperature superimposed on R_{value} results for the 1:30 A.M. AMSRE_{VU} product.

versus P.M. overpass differences in Fig. 5 because the temporal support of A.M. and P.M. R_{value} results may vary. The clearest example of this is the improved performance of all 1:30 P.M. soil moisture products (relative to their A.M. counterparts) over the Tibetan Plateau (see Fig. 5 to the northeast of India). This difference arises because the AMSRE_{VU} and AMSRE_{USDA} products provide only very sporadic 1:30 A.M. retrievals in the region, while all four products provide essentially continuous 1:30 P.M. soil moisture estimates. Because the inclusion of a grid cell on a given day requires the availability of retrievals from all products (in order to make product-to-product comparisons as objective as possible), insufficient A.M. data over the region are available to make robust R_{value} calculations for any product.

VIII. “HOT-SPOT” COMPARISON

For many weather and climate applications, the value of accurate soil moisture retrievals varies geographically. Recent work using an ensemble of climate models has established the concept of soil moisture “hot spots” where soil moisture information is particularly valuable for predicting long-term precipitation and temperature variability [21]. The existence of such discrete areas implies that, for atmospheric predictability applications, these regions should be disproportionately emphasized when globally evaluating a given soil moisture product. Therefore, a fundamental issue for evaluating soil moisture retrievals is the degree to which areas where remote sensing observations add value spatially correspond to identified hot-spot regions.

Fig. 6 examines this issue by overlaying contour lines for precipitation and temperature hot spots predicted by Koster *et al.* [21] on quasi-global R_{value} results for the AMSRE_{VU} A.M.

product. The delineated areas represent the target hot spots where enhanced soil moisture information is particularly relevant for temperature and precipitation forecasting applications. Hot spots generally span transitional regions between humid and arid climates [21]. This tendency is clearly illustrated in central/western North America and sub-Saharan Africa. Within these regions, there is a tendency for the AMSRE_{VU} A.M. product to perform well on the dry side of the climate transition but less successfully on the corresponding wetter side. Future remote sensing measures acquired at L-band have the potential to penetrate further into wetter (and more heavily) vegetated portions of such climate transects. For all the AMSR-E soil moisture products, Fig. 7 shows mean R_{value} results for the following: 1) all global land areas between 50° S and 50° N; 2) only land areas within a precipitation hot spot; and 3) only land areas within a temperature hot spot. R_{value} in hot-spot regions tends to be higher than its global average (see, for example, the AMSRE_{VU} and AMSRE_{USDA} A.M. products). That is, on a globally averaged basis, land cover conditions within hot-spot areas are generally more amenable to soil moisture remote sensing than those outside, and some degree of fortuitous correspondence exists between regions of greatest need and acceptable accuracy for satellite-based surface soil moisture products. However, the R_{value} difference between hot-spot and non-hot-spot areas is not observed in the AMSRE_{SWI} soil moisture product (Fig. 7). This suggests that new areas of soil moisture retrieval skill for 10.6-GHz retrievals (relative to those already observed at 18.7 GHz) tend to be disproportionately located in hot-spot regions. The prospect of preferentially adding retrieval skill within hot-spot regions remains a key motivator for future soil moisture satellite missions based on even lower frequency T_B retrievals [13], [20].

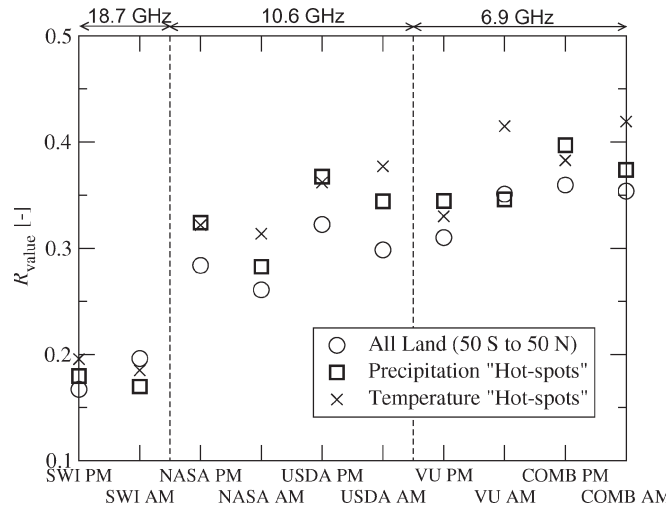


Fig. 7. Spatial average of R_{value} for the AMSRE_{SWI}, AMSRE_{NASA}, AMSRE_{USDA}, AMSRE_{VU}, and AMSRE_{COMB} products for all (circles) land areas between 50° S and 50° N, (squares) land areas within precipitation hot spots, and (crosses) land areas within temperature hot spots.

IX. SUMMARY

To date, designers of soil moisture remote sensing algorithms have generally lacked the ability to evaluate their products at regional and continental scales. Recent research described in [7], [8], and [22] attempts to develop a DA-based approach that spatially expands the geographic extent of regions in which remotely sensed soil moisture products can be evaluated. In this paper, we do the following: 1) Fundamentally modify the existing R_{value} approach (Section II); 2) present the first independent verification of its ability to accurately reproduce validation results obtained over highly instrumented watershed sites; and 3) complete a global-scale application of the newly modified and verified approach.

Watershed verification results demonstrate that the R_{value} metric can effectively mimic correlation-based validation results obtained from dense ground-based soil moisture networks (Fig. 2). In particular, implementation of the methodological modifications introduced in Section II leads to larger R_{value} magnitudes and a stronger correlation with ground-based validation metrics relative to implementation of the baseline approach in [7] and [8] (Table I). This skill in replicating ground-based validation results remains even after input data access is restricted to only satellite-based rainfall data sets (Fig. 3)—suggesting that the R_{value} approach can be effectively applied at global scales. The subsequent application over a quasi-global (50° S–50° N) domain using TMPA precipitation data verifies the expected large-scale tendency for soil moisture retrieval skill to increase as T_B frequency decreases (Fig. 4), and it clarifies the global extent of regions in which remote sensing contributes to the detection of soil moisture anomalies (Fig. 5). The spatial correspondence of these areas with regions of strong land–atmosphere coupling is a critical issue for articulating the value of remotely sensed soil moisture retrievals for atmospheric predictability applications. The results here quantify the degree of overlap between the hot-spot regions identified by Koster *et al.* [21] and those of strong skill for remotely sensed soil moisture products (Figs. 6 and 7).

Despite these results, it is important to note that the R_{value} approach is intended to supplement, and not replace, more traditional satellite soil moisture validation activities based on ground-based soil moisture networks. As noted in [7], the R_{value} metric is blind to bias and/or dynamic range errors and provides only a measure of skill with regard to change detection. While such change-detection skill is frequently cited as the key contribution of remotely sensed soil moisture for many DA activities (see, for example, [9] and [28]), it is not the only metric by which soil moisture products should be validated. In particular, bias and rms error (rmse) calculations must be made versus ground-based observations or through the implementation of an alternative technique designed to recover rmse-type information. A very promising example of such a technique is described by Scipal *et al.* [32]. In addition, the R_{value} metric is most properly interpreted as a measure of added skill, which is sensitive to both the inherent accuracy of a soil moisture product and the accuracy of the rainfall estimates driving a competing water-balance-based estimate of soil moisture (Fig. 2). Such relativity is, of course, a limitation for strict validation activities attempting to establish the absolute accuracy of a given soil moisture product. However, evaluation approaches based on measuring the added value of remotely sensed observations relative to some baseline are important for assessing the higher level value associated with a soil moisture product when assimilated into an existing predictive modeling and/or decision support system.

Follow-on plans for this paper include the application of the technique to L-band soil moisture retrievals obtained from the European Space Agency Soil Moisture and Ocean Salinity mission [20] and integrating the approach into validation plans for the upcoming NASA Soil Moisture Active/Passive mission.

REFERENCES

- [1] P. B. Allen and J. W. Naney, "Hydrology of the Little Washita River Watershed, Oklahoma: Data and analyses," U.S. Dept. Agric., Washington, DC, USDA Tech. Rep. ARS-90, 1991.
- [2] M. C. Anderson, J. M. Norman, J. R. Mecikalski, J. P. Otkin, and W. P. Kustas, "A climatological study of evapotranspiration and moisture stress across the continental U.S. based on thermal remote sensing: II. Surface moisture climatology," *J. Geophys. Res.*, vol. 112, no. D11, p. D11 112, Jun. 2007, DOI: 10.1029/2006JD007507.
- [3] D. D. Bosch, J. M. Sheridan, and L. K. Marshall, "Precipitation, soil moisture, and climate database, Little River Experimental Watershed, Georgia, United States," *Water Resour. Res.*, vol. 43, no. 9, p. W09 472, Sep. 2007, DOI: 10.1029/2006WR005834.
- [4] M. H. Choi, J. M. Jacobs, and D. D. Bosch, "Remote sensing observatory validation of surface soil moisture using Advanced Microwave Scanning Radiometer E, Common Land Model, and ground based data: Case study in SMEX03 Little River Region, Georgia, US," *Water Resour. Res.*, vol. 44, no. 8, p. W08 421, Aug. 2008.
- [5] M. H. Cosh, T. J. Jackson, P. J. Starks, and G. Heathman, "Temporal stability of surface soil moisture in the Little Washita River Watershed and its applications in satellite soil moisture product validation," *J. Hydrol.*, vol. 323, no. 1–4, pp. 168–177, May 2006.
- [6] M. H. Cosh, T. J. Jackson, S. Moran, and R. Bindlish, "Temporal persistence and stability of surface soil moisture in a semi-arid watershed," *Remote Sens. Environ.*, vol. 122, no. 2, pp. 304–313, Feb. 2008.
- [7] W. T. Crow, "A novel method for quantifying value in spaceborne soil moisture retrievals," *J. Hydrometeorol.*, vol. 8, no. 1, pp. 56–57, Feb. 2007.
- [8] W. T. Crow and X. Zhan, "Continental-scale evaluation of spaceborne soil moisture products," *IEEE Geosci. Remote Sens. Lett.*, vol. 4, no. 3, pp. 451–455, Jul. 2007.

- [9] W. T. Crow, R. D. Koster, R. H. Reichle, and H. Sharif, "Relevance of time-varying and time-invariant retrieval error sources on the utility of spaceborne soil moisture products," *Geophys. Res. Lett.*, vol. 32, no. 24, p. L24405, Dec. 2005, DOI: 10.1029/2005GL024889.
- [10] S. Dunne and D. Entekhabi, "An ensemble-based reanalysis approach to land data assimilation," *Water Resour. Res.*, vol. 41, no. 2, p. W02013, Feb. 2005, DOI: 10.1029/2004WR003449.
- [11] S. Dunne, D. Entekhabi, and E. G. Njoku, "Impact of multi-resolution active and passive microwave measurements on soil moisture estimation using the ensemble Kalman smoother," *IEEE Trans. Geosci. Remote Sens.*, vol. 45, no. 4, pp. 1016–1028, Apr. 2007.
- [12] M. Drusch, E. F. Wood, and H. Gao, "Observation operators for the direct assimilation of TRMM Microwave Imager retrieved soil moisture," *Geophys. Res. Lett.*, vol. 32, no. 15, p. L15403, Aug. 2005, DOI: 10.1029/2005GL023623.
- [13] D. Entekhabi, E. Njoku, P. O'Neill, K. Kellogg, W. Crow, W. Edelstein, J. Entin, S. Goodman, T. Jackson, J. Johnson, J. Kimball, J. Piepmeyer, R. Koster, K. McDonald, M. Moghaddam, S. Moran, R. Reichle, J. C. Shi, M. Spencer, S. Thurman, L. Tsang, and J. Van Zyl, "The Soil Moisture Active and Passive (SMAP) mission," *Proc. IEEE*, 2010, to be published.
- [14] A. Gelb, *Applied Optimal Estimation*. Cambridge, MA: MIT Press, 1974.
- [15] D. G. Goodrich, T. O. Keefer, C. L. Unkrich, M. H. Nichols, H. B. Osborn, J. J. Stone, and J. R. Smith, "Long-term precipitation database, Walnut Gulch Experimental Watershed, Arizona, United States," *Water Resour. Res.*, vol. 44, no. 5, p. W05S04, May 2008, DOI: 10.1029/2006WR005782.
- [16] R. W. Higgins, W. Shi, and E. Yarosh, "Improved United States precipitation quality control system and analysis," *NCEP/Climate Prediction Center ATLAS*, vol. 7, p. 40, 2000.
- [17] G. J. Huffman, R. F. Adler, D. T. Bolvin, G. Gu, E. J. Nelkin, K. P. Bowman, Y. Hong, E. F. Stocker, and D. B. Wolff, "The TRMM Multisatellite Precipitation Analysis: Quasi-global, multiyear, combined-sensor precipitation estimates at fine scale," *J. Hydrometeorol.*, vol. 8, no. 1, pp. 28–55, Feb. 2007.
- [18] T. J. Jackson, "Measuring surface soil moisture using passive microwave remote sensing," *Hydrolog. Process.*, vol. 7, no. 2, pp. 139–152, 1993.
- [19] T. J. Jackson, M. Cosh, R. Bindlish, P. Starks, D. Bosch, M. Seyfried, D. Goodrich, S. Moran, and D. Du, "Validation of Advanced Microwave Scanning Radiometer soil moisture products," *IEEE Trans. Geosci. Remote Sens.*, 2010, to be published.
- [20] Y. H. Kerr and D. Levine, "Forward to the special issue on the Soil Moisture and Ocean Salinity (SMOS) mission," *IEEE Trans. Geosci. Remote Sens.*, vol. 46, no. 3, pp. 583–585, Mar. 2008.
- [21] R. D. Koster, Y. C. Sud, Z. Guo, P. A. Dirmeyer, G. Bonan, K. W. Oleson, E. Chan, D. Verseghy, P. Cox, H. Davies, E. Kowalczyk, C. T. Gordon, S. Kanae, D. Lawrence, P. Liu, D. Mocko, C.-H. Lu, K. Mitchell, S. Malyshev, B. McAvaney, T. Oki, T. Yamada, A. Pitman, C. M. Taylor, R. Vasic, and Y. Xue, "GLACE: The global land-atmosphere coupling experiment. Part I: Overview," *J. Hydrometeorol.*, vol. 7, no. 4, pp. 590–710, Aug. 2006.
- [22] A. Loew, M. Schwank, and F. Schlenz, "Assimilation of an L-band microwave soil moisture proxy to compensate for uncertainties in precipitation data," *IEEE Trans. Geosci. Remote Sens.*, vol. 47, no. 8, pp. 2606–2616, Aug. 2009.
- [23] E. G. Njoku, T. J. Jackson, V. Lakshmi, T. Chan, and S. V. Nghiem, "Soil moisture retrieval from AMSR-E," *IEEE Trans. Geosci. Remote Sens.*, vol. 41, no. 2, pp. 215–229, Feb. 2003.
- [24] E. G. Njoku, P. Ashcroft, T. K. Chan, and L. Li, "Global survey and statistics of radio-frequency interference in AMSR-E land observations," *IEEE Trans. Geosci. Remote Sens.*, vol. 43, no. 5, pp. 938–947, May 2005.
- [25] E. G. Njoku, *AMSR-E/Aqua Daily L3 Surface Soil Moisture, Interpretive Parameters, and QC EASE-Grids*, Boulder, CO: Nat. Snow Ice Data Center, 2008, July 2002 to December 2007, daily updated digital media.
- [26] M. Owe, R. A. M. de Jeu, and T. H. R. Holmes, "Multisensor historical climatology of satellite-derived global land surface soil moisture," *J. Geophys. Res.*, vol. 113, no. F1, p. F01002, Jan. 2008, DOI: 10.1029/2007JF000769.
- [27] H. E. Rauch, F. Tung, and C. T. Striebel, "Maximum likelihood estimates of linear dynamic systems," *AIAA J.*, vol. 3, no. 8, pp. 1445–1450, Aug. 1965.
- [28] R. H. Reichle, W. T. Crow, R. D. Koster, H. Sharif, and S. Mahanama, "Contribution of soil moisture retrievals to land data assimilation products," *Geophys. Res. Lett.*, vol. 35, no. 1, p. L01404, Jan. 2008, DOI: 10.1029/2007GL031986.
- [29] K. G. Renard, M. H. Nichols, D. A. Woolhiser, and H. B. Osborn, "A brief background on the U.S. Department of Agriculture Agricultural Research Service Walnut Gulch Experimental Watershed," *Water Resour. Res.*, vol. 44, p. W05S02, May 2008, DOI: 10.1029/2006WR005691.
- [30] R. Panciera, J. P. Walker, J. D. Kalma, E. J. Kim, J. M. Hacker, O. Merlin, M. Berger, and N. Skou, "The NAFE'05/Cosmos data set: Toward SMOS soil moisture retrieval, downscaling, and assimilation," *IEEE Trans. Geosci. Remote Sens.*, vol. 46, no. 3, pp. 736–745, Mar. 2008.
- [31] A. K. Sahoo, P. R. Houser, C. Ferguson, E. F. Wood, P. A. Dirmeyer, and M. Kafatos, "Evaluation of AMSR-E soil moisture results using the in *in-situ* data over the Little River Experimental Watershed," *Remote Sens. Environ.*, vol. 112, no. 6, pp. 3142–3152, Jun. 2008.
- [32] K. Scipal, T. Holmes, R. de Jeu, V. Naeimi, and W. Wagner, "A possible solution for the problem of estimating the error structure of global soil moisture datasets," *Geophys. Res. Lett.*, vol. 35, no. 24, p. L24403, Dec. 2009, DOI: 10.1029/2008GL035599.
- [33] R. Scofield, J. G. LaDue, R. Scofield, N. Grody, and R. Ferraro, "A soil wetness index for monitoring the great flood of 1993," in *Proc. 7th Conf. Satell. Meteorol. Oceanography*, 1994, pp. 580–583.
- [34] H. Van Storch and F. W. Zwiers, *Statistical Climatology*. Cambridge, U.K.: Cambridge Univ. Press, 2002.
- [35] V. Naeimi, K. Scipal, Z. Bartalis, S. Hasenauer, and W. Wagner, "An improved soil moisture retrieval algorithm for ERS and METOP scatterometer observations," *IEEE Trans. Geosci. Remote Sens.*, vol. 47, no. 7, pp. 1999–2013, Jul. 2009.
- [36] W. Wagner, V. Naeimi, K. Scipal, R. De Jeu, and J. M. Fernandez, "Soil moisture from operational meteorological satellites," *Hydrogeology*, vol. 15, no. 1, pp. 121–131, Feb. 2007.
- [37] M. Zribi, C. Andre, and B. Decharme, "A method for soil moisture estimation in Western Africa based on the ERS scatterometer," *IEEE Trans. Geosci. Remote Sens.*, vol. 46, no. 2, pp. 438–448, Feb. 2008.



Wade T. Crow (M'03) received the Ph.D. degree from Princeton University, Princeton, NJ, in 2001.

He is currently a Research Physical Scientist with the Hydrology and Remote Sensing Laboratory, Agricultural Research Service, U.S. Department of Agriculture, Beltsville, MD. His research involves the development of land data assimilation techniques to enhance the utility of remote sensing observations for hydrologic and agricultural applications.



Diego G. Miralles received the B.S. degree in environmental sciences from the Autonomous University of Madrid, Madrid, Spain, in 2005 and the M.S. degree in hydrology from Vrije University, Amsterdam, The Netherlands, in 2008, where he is currently working toward the Ph.D. degree in the Department of Hydrology, with his research focusing on the development of a new remotely sensed global evaporation product.

From mid-2008 to early 2009, he was a Visiting Scientist at the Hydrology and Remote Sensing Research Laboratory, Agricultural Research Service, U.S. Department of Agriculture, Beltsville, MD.



Michael H. Cosh received the Ph.D. degree from Cornell University, Ithaca, NY, in 2002, when he joined the Agricultural Research Service (ARS).

He is currently a Research Hydrologist with the Hydrology and Remote Sensing Laboratory, ARS, U.S. Department of Agriculture, Beltsville, MD. His research involves the scaling of *in situ* ground data to remote sensing scales, spatial variability assessment of soil moisture, and developing methods to establish long-term validation sites for remote sensing platforms, including the use of temporal and spatial

stability.